Hierarchical Nanotextured Microelectrodes Overcome the Molecular Transport Barrier To Achieve Rapid, Direct Bacterial Detection

Leyla Soleymani,[†,∥] Zhichao Fang,[‡,∥] Brian Lam,[§] Xiaomin Bin,[†] Elizaveta Vasilyeva,[⊥] Ashley J. Ross,[‡] Edward H. Sargent,[†,*] and Shana O. Kelley[‡,§,⊥,*]

[†]Department of Electrical and Computer Engineering, Faculty of Engineering, [‡]Department of Pharmaceutical Sciences, Leslie Dan Faculty of Pharmacy, [§]Department of Chemistry, Faculty of Arts and Sciences, and [⊥]Department of Biochemistry, Faculty of Medicine, University of Toronto, Ontario, Canada [∥] These authors contributed equally to this work.

ABSTRACT Detection of biomolecules at low abundances is crucial to the rapid diagnosis of disease. Impressive sensitivities, typically measured with small model analytes, have been obtained with a variety of nano- and microscale sensors. A remaining challenge, however, is the rapid detection of large native biomolecules in real biological samples. Here we develop and investigate a sensor system that directly addresses the source of this challenge: the slow diffusion of large biomolecules traveling through solution to fixed sensors, and inefficient complexation of target molecules with immobilized probes. We engineer arrayed sensors on two distinct length scales: a ~100 μm length scale commensurable with the distance bacterial mRNA can travel in the 30 min sample-to-answer duration urgently required in point-of-need diagnostic applications; and the nanometer length scale we prove necessary for efficient target capture. We challenge the specificity of our hierarchical nanotextured microsensors using crude bacterial lysates and document the first electronic chip to sense trace levels of bacteria in under 30 min.

KEYWORDS: biosensing · nanomaterials · bacterial detection · pathogen detection · electrochemical sensors

Over the past decade, a variety of elegant systems for the detection of nucleic acids and other biomolecular analytes have emerged.[1−10] Such efforts aim to achieve miniaturized, cost-effective diagnostic devices for rapid medical and environmental monitoring.[11,12] Chip-based approaches are particularly attractive for diagnostic device development and, therefore, remain of great interest.

While nano- and microscale sensing elements have been found to improve dramatically the limit of detection of a biosensing system when model analytes are used (*e.g.*, synthetic oligonucleotides),[1−10] this has not led to success with the ultrasensitive detection of native nucleic acids (*e.g.*, mRNAs). This limitation reflects the challenge of using small sensors to capture very slow moving large molecules. For example, our laboratory recently described chip-based microsensors that achieved high sensitivities and detected specific DNA oligonucleotides at attomolar concentrations.[13−15] However, when attempting to detect biologically relevant nucleic acids such as mRNA sequences,[16] detection limits were significantly degraded. While tumor RNA could still be profiled, this loss in sensitivity precluded the use of the device for direct detection of nucleic acids in clinically relevant samples where lower concentrations of analytes are available.

The size/sensitivity/speed trade-off in biomolecular detection is well-documented and has been modeled extensively.[17−21] Much of this work has focused on how sensor size affects detection times for small analytes[18] or how nanoscale sensor geometry affects detection times,[19] with less attention paid to the detection of large analytes of critical interest, such as mRNAs. Moreover, despite thoughtful explorations of the constraints that molecular diffusion imposes on the analysis of clinical samples,[20,21] and the development of intuitive models describing how flux, time, and sensor size affect detection performance,[17] there is a dearth of experimental work that attempts to overcome diffusional barriers in passive solutions. Given the attractiveness of automation-friendly chip-based devices for diagnostic applications—devices further simplified when active solution transport is not mandated to speed molecular transport—we

* Address correspondence to shana.kelley@utoronto.ca, ted.sargent@utoronto.ca.

Received for review February 13, 2011 and accepted March 16, 2011.

Published online March 16, 2011
10.1021/nn200586s

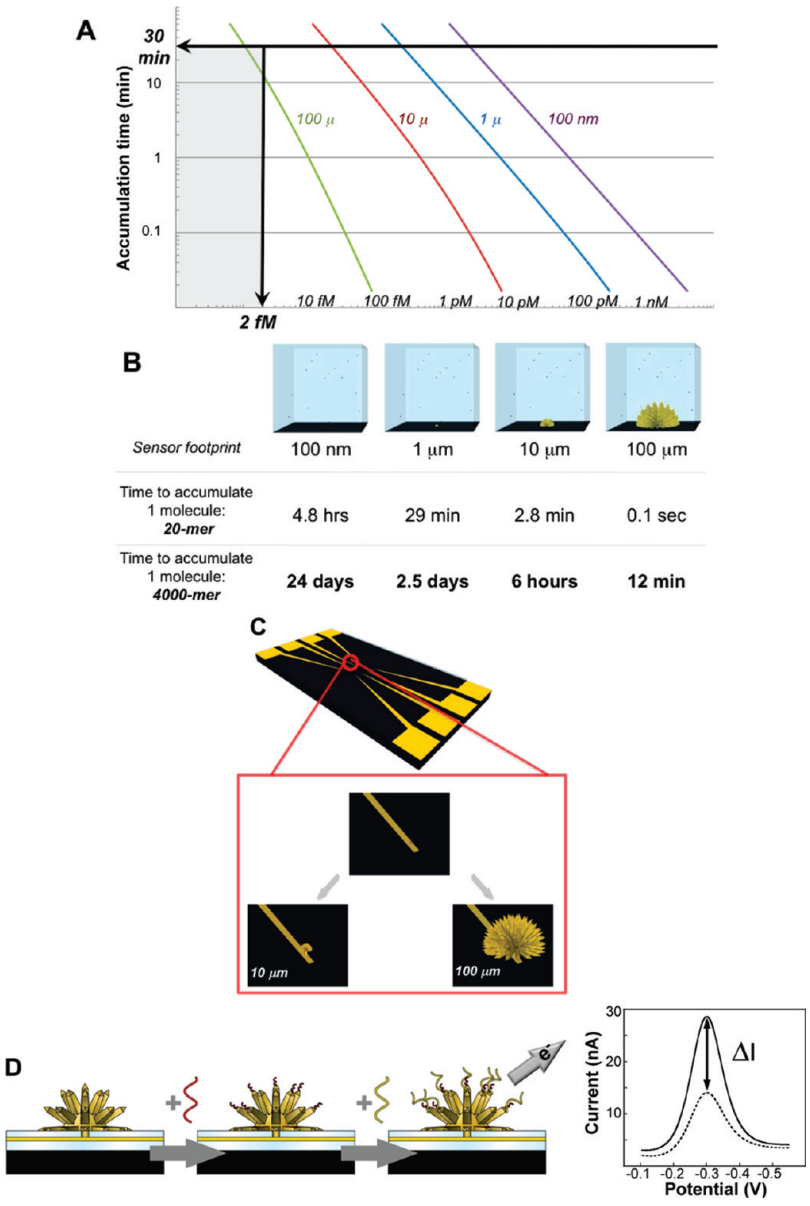

Figure 1. (A,B) Results of computational analysis of structure size *versus* time required to accumulate one molecule in a solution containing 2 fM of a nucleic acids target. The model used to calculate these values is described in detail in the Supporting Information. The effects of sensor size, analyte concentration, and analyte size were studied to identify the direct measurement of mRNA. (C) Approach to developing arrayed micrometer scale sensors for detection of large bacterial targets. Sensors of variable sizes were electrodeposited on gold leads with a top layer of SiO_2 with 5 μm pores positioned at the ends of gold leads. (D) Preparation and use of microsensors. After electrodeposition, sensors were modified with probe molecules (red) complementary to a target bacterial gene (yellow). After hybridization, sensors were interrogated using the electrocatalytic reporter system described in ref 27. The change in current upon hybridization with an analyte was assessed by measuring differential pulse voltammograms and quantitating peak currents before (dotted line) and after (solid line) incubation.

explored whether it might be possible to render direct mRNA detection feasible using arrayed sensors that take into consideration the slow diffusion of native biomolecules.

To assess the ideal size scale for sensors capable of detecting native mRNAs in clinical samples, we performed a series of calculations (Figure 1). Using existing models described by Sheehan/Whitman[18] and Nair/Alam[19] that analyze molecular diffusional behavior, we assessed the time dependence of analyte accumulation on sensors of varying sizes. The times required for accumulation of one molecule from a 2 fM solution on sensors of different sizes was compared for a 20 base oligonucleotide and a 4000 nucleotide mRNA. The concentration for the calculations was derived from choosing a copy number of 1400 of the target mRNA and a clinically relevant concentration of bacteria of 100 cells in 100 μL (this is what is contained in most clinical swab samples). If a 30 min cutoff time is imposed, it is clear that a sensor with a hemispherical footprint of at least 100 μm is required to capture one molecule within this window.

It is clear that for both the model analyte (20-mer) and the native mRNA (4000-mer), nanoscale sensors cannot be used for rapid (<30 min) testing. For the mRNA analyte, a 100 μm sensor would allow significant accumulation of a 4000 base target within 30 min. A sensor with this footprint would reach into the sample droplet, ensuring that many more molecules are proximate to the sensor surface.

The conclusion that microscale sensors are needed for rapid detection holds even when flow or active transport of target molecules is considered (see Supporting Information Figure S2). For example, a 100 nm sensor, capable only of detecting large analytes in 100 pM solutions within 30 min, only improves its sensitivity by a factor of 10 when solution is flowed past it at a fast rate (20 μL/min). For small sensors, the enhancement is even smaller and cannot speed the accumulation of dilute, large molecules. Alternatively, it could be envisioned that electrokinetic transport could draw large molecules toward a sensor at an accelerated rate. However, the strong fields required are problematic when coupled with ultrasensitive detection systems and introduce limitations in sample composition. Thus, while active transport can speed mass transport, it is worthwhile to solve the passive transport problem in order to facilitate the development of simple, practical sensing devices.

The question thus arises: can one meet the rapid sensing challenge by building a robust 3D sensor that reaches many micrometers into solution, while still maintaining the very high level of sensitivity that will be necessary to detect biomolecules such as large nucleic acids at relevant concentrations? We explored this possibility by using a micropatterned substrate to grow sensors (Figure 1C) into solution. Drawing on prior work in our laboratories demonstrating that 5 μm structures could be made by depositing metal into templated apertures in a SiO_2 layer,[13−16] we explored whether electrodeposition could be used to generate sensors with the 100 μm footprint that was identified as critical in our calculations. Electrodeposition has been used extensively to create 2D nanostructures,[22] or coat surfaces with a nanostructured layer,[23] but has never been used to make unsupported, isolated structures 100 μm high, presenting an interesting challenge to the use of the approach.

A variety of materials and deposition conditions were tested in order to provide access to the large structures desired. Gold was identified as a metal that would facilitate the growth of the electrodes 100 μm into solution; in contrast, metals like palladium produced structures that extended only a few micrometers vertically and primarily grew along the chip surface horizontally (Figure 2). High plating potentials and metal salt concentrations—conditions that drive fast and fractal growth of metal structures—facilitated successful fabrication of the desired gold structures. It

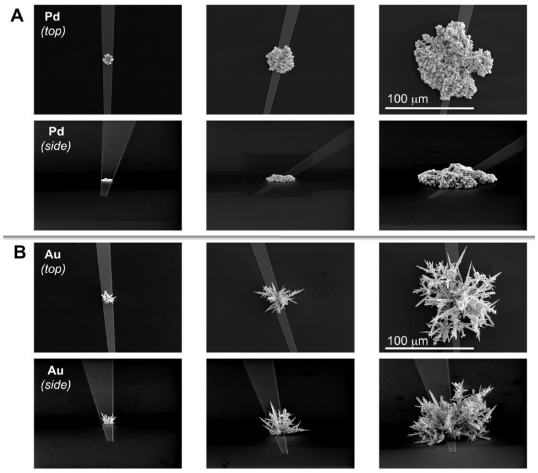

Figure 2. Development of approach to generate 3D sensors with 100 μm footprint. (A) Electrodeposition of palladium was performed using a voltage of −250 mV for 20 (left), 100 (middle), and 360 s (right). (B) Electrodeposition of gold was performed using a voltage of 0 mV for 30 (left), 90 (middle), 240 s (right). See Supporting Information for all fabrication procedures.

is notable that these sensors, which are fractal in nature and therefore exhibit small morphological differences from sensor to sensor, exhibit very reproducible and controllable properties (see Supporting Information Figures S4 and S5) because electrodeposition allows fine control over nanoscale surface morphology and overall surface area.

Previous work in our laboratories suggested that nanoscale roughness of an electrode surface can significantly improve biosensing limit of detection.[13,14] However, as seen in Figure 3A, our ∼100 μm sized sensors were substantially smooth on length scales shorter than 100 nm. While the choice of gold as a sensor material allowed us to reach our goal of making structures that protrude out into solution to promote target capture, this material did not produce the nanoscale features that would enhance probe display. We were thus motivated to find a means to generate nanoscale roughness on these structures in the hope of further increasing sensitivity.

We were able to introduce a thin nanostructured overcoating of palladium on the surfaces of the gold microstructures using electrodeposition; palladium is particularly versatile in producing different nanostructured morphologies depending on deposition conditions.[23] As shown in Figure 3B, this produced a layer of nanostructures ranging from 10 to 50 nm and a hierarchical nanostructured microsensor structure (HNME) with size features spanning the microscale to nanoscale.

We assessed DNA probe coverage and the efficiency of hybridization with a synthetic target on microsensors with and without nanostructuring and found that the presence of the nanostructured layer had a large

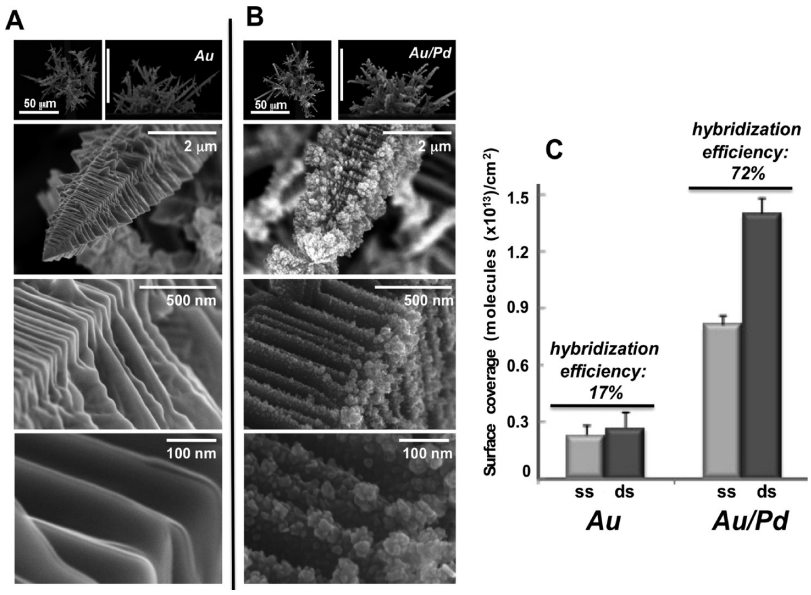

Figure 3. Effect of nanostructuring HNMEs. As shown in (A), microstructures made from Au alone did not exhibit significant nanoscale roughness. Only with electrodeposition of a fine layer of Pd (B) was roughness on the length scale of 10−50 nm achieved. The introduction of this layer and the generation of hierarchical nanotextured microelectrodes (HNMEs) increased the surface coverage of immobilized DNA single-stranded (ss) probe molecules and greatly enhanced the efficiency of hybridization of a synthetic complementary sequence (ds), as evaluated using a chronocoulometric assay and shown in (C). Sequences used in this analysis were DP-EC and C-DP-EC.

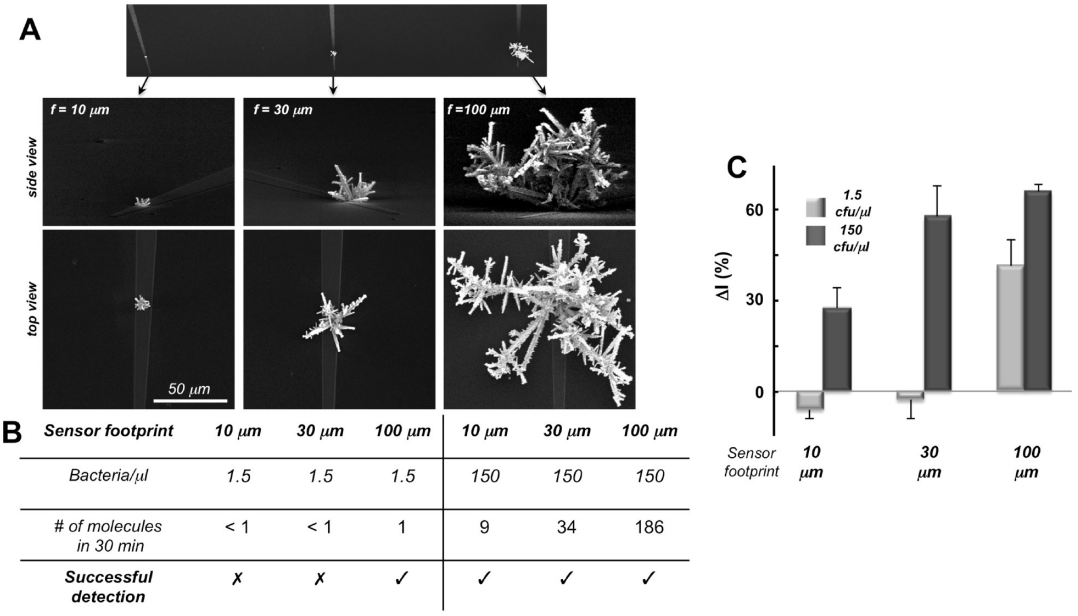

B

Sensor footprint	10 μm	30 μm	100 μm	10 μm	30 μm	100 μm
Bacteria/μl	1.5	1.5	1.5	150	150	150
# of molecules in 30 min	< 1	< 1	1	9	34	186
Successful detection	✗	✗	✓	✓	✓	✓

Figure 4. Validation of required sensor footprint for bacterial detection in 30 min. (A) Variation of sensor size. To test whether the sensitivities of the detectors to bacterial lysates, sensors with three different sizes were generated (10, 30, and 100 μm) and modified with the DP-EC probe. (B) Data summary from testing of sensors with lysates of solutions of E. coli containing either 1.5 or 150 cfu per microliter. DNA probe modified HNMEs were challenged with unpurified lysates generated from varying numbers of bacteria, and signals were collected in the presence of an electrocatalytic Ru(III)/Fe(III) reporter system. (C) Representative data used to evaluate limits of detection. Δ*I* values were extracted from differential pulse voltammetry curves, and a noncomplementary probe was used to evaluate background signals.

effect (Figure 3C). Using an assay based on $Ru(NH_3)_6^{3+}$ adsorption,[24] the density of an adsorbed DNA probe and the number of probes that hybridized with a synthetic complement were measured. With the increased nanostructuring, probe surface coverage *and* the hybridization efficiency improved dramatically. The enhanced probe density likely arises from the presence of smaller nanostructures that increase the deflection angle between probes and allow them to form more dense monolayers.[25] This increased deflection angle then provides better access for incoming target molecules.[26]

With these large structures in hand, we sought to explore their performance when presented with mRNAs specific to bacterial cells. The rapid detection and classification of bacteria represents an unmet need in medicine that could greatly benefit from the type of direct detection our calculations indicated could be performed in 30 min or less with the chip-based sensors. To detect specific bacterial sequences with the sensors, we derivatized the microscaffolds with thiol-terminated single-stranded probe sequences (Figure 1D) and employed an electrocatalytic assay[27] for readout. The probe was made complementary to the RNA polymerase β mRNA (*rpoB*), a transcript with a high expression level in bacteria[28] that has a sequence exhibiting significant variation from species to species, making it an ideal target for bacterial detection and identification.

HNME sensors of three different sizes (10, 30, and 100 μm) were then tested to determine whether the 100 μm sensor footprint was indeed necessary to meet our detection challenge (Figure 4A). The sensors were incubated with solutions of unpurified bacterial lysates generated from cultured *Escherichia coli* using a reagent-free approach that relies on a rapid (<1 min) electrical lysis technique amenable to in-line integration with electronic chips.[29] Indeed, the 100 μm HNME did exhibit the level of sensitivity desired when tested with crude *E. coli* extracts (Figure 4B,C). While the 10 and 30 μm sensors were effective at detecting bacterial concentrations 100-fold higher, they could not produce a detectable response with the lower concentrations. Negative signals were observed when these sensors were incubated with the bacterial lysates. These negative signal changes were most pronounced when small sensors were used, likely because the small background currents observed were more easily perturbed when cellular components interacted with the sensors nonspecifically. Larger structures could also be generated using the same approach. However, background currents increased with increasing size. Therefore, we did not use larger structures for sensing as we met our speed and sensitivity goals with 100 μm structures.

The results reported here represent an important advance in the development of electrochemical biosensing systems. Our previous work showed that highly sensitive, multiplexed sensors could be generated using straightforward lithographic fabrication and electrodeposition.[13−16] However, we discovered that the low limits of detection measured with small oligonucleotides were not maintained when large nucleic acids molecules, like mRNAs, were monitored. As demonstrated here, the larger analytes require larger sensors in order to promote collision between the sensor and target molecule. The need for nanostructured surfaces noted previously[13] remains, as we report here that hybridization efficiencies for 100 μm sensors are optimal if a nanostructured layer of metal is introduced on the surface of the large microstructure. Clearly, two distinct length scales are of key importance in the development of effective biosensors: (1) The nanostructuring length scale in the 1−30 nm range. This length scale of surface roughness is responsible for the efficiency display of the probe monolayer and is necessary to achieve high-efficiency hybridization with the target. (2) The largest macroscopic extent of the electrode. This length scale, taken together with the diffusion length of target molecules of interest, determines the volume of solution that the electrode can interact with within the finite hybridization time. We found that structures with a footprint of ~100 μm were optimal. Thus, structures with a range of 3000−10 000× variation in feature size are most effective for biomolecular detection.

Excellent detection limits have been achieved with electrochemical detection schemes previously.[6,30] Prior studies, however, only tested small, synthetic oligonucleotides as analytes, and therefore, it is unclear that they would maintain high levels of sensitivity with native nucleic acids in the unpurified samples being tested here. The ability to analyze heterogeneous samples and directly detect naturally occurring sequences with little sample processing is an important advance. The approach is highly versatile and appropriate for bacterial detection as described here or the analysis of cancer biomarkers in human cells.[31]

METHODS

Preparation and Purification of Oligonucleotides. DNA sequences were obtained from the Centre for Applied Genomics in the Hospital for Sick Children (Toronto, Canada). Modification of DNA oligonucleotides on the 5′-terminus with a hexanediamine-based linker was described previously.[7] The following probe and target sequences were used in experiments. **Seq. DP-EC** (DNA probe for *E. coli*): $^{5'}$ATCTGCTCTGTGGTGTAGTT$^{3'}$, **Control probe**: $^{5'}$AAGTAAGACATTGATGCAAT$^{3'}$, Complement to DP-EC (**C-DP-EC**): $^{5'}$AACTACACCACAGAGCAGAT$^{3'}$. Oligonucleotides were quantitated by measuring absorbance at 260 nm. Extinction coefficients of DNA probes were obtained using http://www.idtdna.com/analyzer/Applications/OligoAnalyzer/.

Chip Fabrication. The chips were fabricated at the Canadian Photonics Fabrication Center. Six inch silicon wafers were passivated using a thick layer of thermally grown silicon dioxide. A 300 nm gold layer was deposited on the chip using electron-beam-assisted gold evaporation. Gold film was patterned using standard photolithography and a lift-off process. A 500 nm layer of insulating silicon dioxide was deposited using chemical vapor deposition. Then, 500 nm or 5 μm apertures were imprinted on the electrodes using standard photolithography. In addition, 2 mm × 2 mm bond pads were exposed using standard photolithography.

Fabrication of Hierarchical Nanotextured Microelectrodes (HNMEs). Fabricated chips were cleaned by sonicating in acetone and rinsing in IPA followed by DI water for 30 s and dried with a flow of nitrogen. All electrodeposition was performed at room temperature using a Bioanalytical Systems Epsilon potentiostat in a three-electrode configuration featuring an Ag/AgCl reference electrode and a platinum wire auxiliary electrode. Five micrometer apertures in the case of large HNMEs and 500 nm apertures in the case of small HNMEs served as working electrodes and were contacted using the exposed bond pads. Large gold HNMEs with no palladium coating were plated on 5 μm apertures in an aqueous solution containing 20 mM $HAuCl_4$ and 0.5 M HCl at 0 mV for 300 s. Large gold HNMEs with a Pd coating were fabricated using the same procedures as the large gold HNME followed by rinsing with DI water and drying. Such gold structures were then replated in a solution of 5 mM H_2PdCl_4 and 0.5 M $HClO_4$ at -250 mV for 10 s. Small HNMEs were fabricated on 500 nm apertures in an aqueous solution containing 20 mM $HAuCl_4$ and 0.5 MHCl and were plated at 0 mV for 50 s.

Modification of HNMEs with DNA Probes. HNMEs prepared as described above were cycled in 0.05 M H_2SO_4 from 0 to $+1465$ mV for 10 cycles. Following the acid cleaning, 10 μL of solution containing 5 μM thiolated single-stranded DNA, 1 mM magnesium chloride, 25 mM sodium phosphate (pH 7), and 25 mM sodium chloride were deposited on the HNMEs in a dark humidity chamber for 30 min at room temperature. The HNMEs were then rinsed in 25 mM sodium phosphate (pH 7), 25 mM NaCl buffer. The adsorption of DNA on the HNMEs surface was confirmed by monitoring the attenuation of the electrochemical signal obtained from a solution of 10 mM ferrocyanide in 25 mM sodium phosphate (pH 7) and 25 mM NaCl solution (data not shown).

Electrochemical Measurements. Electrochemical signals were measured in solutions containing 10 μM $Ru(NH_3)_6^{3+}$, 4 mM $Fe(CN)_6^{3-}$ with a buffer of 25 mM sodium phosphate (pH 7), and 25 mM sodium chloride. Cyclic voltammetry signals before and after hybridization were collected with a scan rate of 100 mV/s. Limiting reductive current (I) was quantified by subtracting the background at 0 mV from the cathodic current at -300 mV in a cyclic voltammetry signal. Differential pulse voltammetry (DPV) signals before and after hybridization were measured using a potential step of 5 mV, pulse amplitude of 50 mV, pulse width of 50 ms, and a pulse period of 100 ms. Signal changes corresponding to hybridization were calculated as follows: $\Delta I = (I_{ds} - I_{ss})/I_{ss} \times 100\%$ (ss = before hybridization, ds = after hybridization) and normalized to the maximal response of a specific device type. Detection limit was called as the first concentration where background (noncomplementary ΔI) subtracted signal was 3 times higher than the standard deviation at that concentration. At least six independent trials were used to generate each data set described in the article.

Bacterial Lysate Hybridization Protocol. Hybridization solutions were bacterial lysates in 1$\times$ sterile PBS (pH 7.4). Electrodes were incubated at 37 °C in a dark humidity chamber for 30 min and were washed extensively with buffer before electrochemical analysis. Hybridization was performed in 10 μL volume.

Surface Coverage and Hybridization Efficiency Analysis. The ssDNA surface coverage of Au HNMEs and Pd-coated Au HNMEs was determined using a chronocoulometric method based on that reported by Steel *et al.*[24] The ssDNA functionalized HNMEs first immersed in 25/25 pure electrolyte buffer, the potential stepped from $+0.15$ to -0.45 V *versus* Ag/AgCl for 200 ms, and the resulting charge flow was measured. The electrode was then immersed in a solution of 50 μM hexaammineruthenium-(III) chloride ($Ru(NH_3)_6^{3+}$) in 25/25 buffer, and the measurement was repeated. Both solutions were purged with argon for at least 20 min prior to the experiment. In the low ionic strength buffer, the trivalent $Ru(NH_3)_6^{3+}$ preferentially exchanges with the native monovalent DNA counterions until they are essentially completely replaced, electrostatically associating with the singly negatively charged DNA phosphate groups in the ratio 1:3. Hybridization analysis used C-DP-EC as a synthetic complement, and hybridization was performed as described above.

Lysis of Bacterial Samples. Electrical bacterial lysis was achieved using an approach similar to that reported by Chang and coworkers.[29] Solutions of *E. coli* were suspended in 1$\times$ saline PBS (pH 7.4), and electrical lysis was achieved using a flow rate of 20 L/min (achieved with a syringe pump) and application of 400 V within a micro/nanochannel device. Static devices consisting of 2 cm $\times$ 2 cm $\times$ 200 μm chamber with 4 cm^2 electrodes as walls and no flow also were effective for lysis with an applied voltage of 50 V for 10 s.

Absolute Quantification of rpoB Transcripts. *Generation of RNA for Standard Curve.* Total RNA was isolated from an overnight *E. coli* culture (Invitrogen), and a reverse transcription reaction was performed to generate a 185 bp cDNA (Qiagen). It was subsequently cloned into a PCR-4 TOPO vector and transformed into competent *E. coli* cells (Invitrogen). After amplification in the *E. coli* cells, vectors were isolated and linearized with *NcoI* endonuclease. After sequencing of the vector was done to determine orientation of the insert, RNA (2751 bp) was transcribed using a T7 *in vitro* transcription system (Epicenter). Integrity of RNA was checked using gel elecrophoresis, and concentration of the sample was determined by measuring the absorbance at 260 nm (A260) in a spectrophotometer.

Real-Time RT-PCR. Standard quantities were prepared over a 5-log range. Unknown samples were prepared by lysing overnight culture of *E. coli* in a lysis chamber. Undiluted 1:100 and 1:10 000 samples lysed bacteria were used to determine the absolute number of the rpoB transcripts. One-step RT-PCR was run according to the manufactures protocol (*Power* SYBR Green RNA-to-CT *1-Step*, Applied Biosystems). All samples were run in triplicate.

Acknowledgment. We wish to acknowledge Genome Canada, the Ontario Institute for Genomics, the Ontario Ministry of Research and Innovation, NSERC, CIHR, Ontario Centres for Excellence, and the Canada Research Chairs Program. In addition, we thank Chang Lu of Virginia Tech for an initial supply of lysis devices and George Pampalakis of the University of Patras for assistance with probe design.

Supporting Information Available: Supporting figures. This material is available free of charge *via* the Internet at http://pubs.acs.org.

REFERENCES AND NOTES

1. Zheng, G.; Patolsky, F.; Cui, Y.; Wang, W. U.; Lieber, C. M. Multiplexed Electrical Detection of Cancer Markers with Nanowire Sensor Arrays. *Nat. Biotechnol.* **2005,** *23*, 1294–1301.
2. Yi, M. Q.; Jeong, K. H.; Lee, L. P. Theoretical and Experimental Study Towards a Nanogap Dielectric Biosensor. *Biosens. Bioelectron.* **2005,** *20*, 1320–1326.
3. Vlassiouk, I.; Kozel, T.; Siwy, Z. Biosensing with Nanofluidic Diodes. *J. Am. Chem. Soc.* **2009,** *131*, 8211–8220.
4. Star, A.; Tu, E.; Niemann., J.; Gabriel, J.-C. P.; Joiner, C. S.; Valcke, C. Label-Free Detection of DNA Hybridization Using Carbon Nanotube Network Field-Effect Transistors. *Proc. Natl. Acad. Sci. U.S.A.* **2006,** *103*, 921–926.
5. Park, S. J.; Taton, T. A.; Mirkin, C. A. Array-Based Electrical Detection of DNA with Nanoparticle Probes. *Science* **2002,** *295*, 1503–1506.
6. Munge, B.; Liu, G. D.; Collins, G.; Wang, J. Multiple Enzyme Layers on Carbon Nanotubes for Electrochemical Detection Down to 80 DNA Copies. *Anal. Chem.* **2005,** *77*, 4662–4666.
7. Li, J.; Ng, H. T.; Cassell, A.; Fan, W.; Chen, H.; Ye, Q.; Koehne, J.; Han, J.; Mayyappan, M. Carbon Nanotube Nanoelectrode Array for Ultrasensitive DNA Detection. *Nano Lett.* **2003,** *3*, 597–602.
8. Hahm, J.; Lieber, C. M. Direct Ultrasensitive Electrical Detection of DNA and DNA Sequence Variations Using Nanowire Nanosensors. *Nano Lett.* **2004,** *4*, 51–54.
9. Cui, Y.; Wei, Q.; Park, H.; Lieber, C. M. Nanowire Nanosensors for Highly Sensitive and Selective Detection of Biological and Chemical Species. *Science* **2001,** *293*, 1289–1292.

10. Ke, Y.; Lindsay, S.; Chang, Y.; Liu, Y.; Yan, H. Self-Assembled Water-Soluble Nucleic Acid Probe Tiles for Label-Free RNA Hybridization Assays. *Science* **2008,** *319*, 180–183.
11. Walt, D. R. Miniature Analytical Methods for Medical Diagnostics. *Science* **2005,** *308*, 217–219.
12. Rosi, N. L.; Mirkin, C. A. Nanostructures in Biodiagnostics. *Chem. Rev.* **2005,** *105*, 1547–1562.
13. Soleymani, L.; Fang, Z.; Sargent, E. H.; Kelley, S. O. Programming the Detection Limits of Biosensors through Controlled Nanostructuring. *Nat. Nanotechnol.* **2009,** *4*, 844–848.
14. Soleymani, L.; Fang, Z.; Sun, X.; Yang, H.; Taft, B. J.; Sargent, E. H.; Kelley, S. O. Nanostructuring of Patterned Microelectrodes To Enhance the Sensitivity of Electrochemical Nucleic Acids Detection. *Angew. Chem., Int. Ed.* **2009,** *121*, 8609–8612.
15. Yang, H.; Hui, A.; Pampalakis, G.; Soleymani, L.; Liu, F.-F.; Sargent, E. H.; Kelley, S. O. Direct Electronic MicroRNA Detection for the Rapid Determination of Differential Expression Profiles. *Angew. Chem., Int. Ed.* **2009,** *48*, 8461–8464.
16. Fang, Z.; Soleymani, L.; Pampalakis, G.; Yoshimoto, M.; Squire, J. A.; Sargent, E. H.; Kelley, S. O. Direct Profiling of Cancer Biomarkers in Tumor Tissue Using a Multiplexed Nanostructured Microelectrode Integrated Circuit. *ACS Nano* **2009,** *3*, 3207–3213.
17. Squires, T. M.; Messinger, R. J.; Manalis, S. R. Making It Stick: Convection, Reaction and Diffusion in Surface-Based Biosensors. *Nat. Biotechnol.* **2008,** *26*, 417–426.
18. Sheehan, P. E.; Whitman, L. J. Detection Limits for Nanoscale Biosensors. *Nano Lett.* **2005,** *5*, 803–807.
19. Nair, P. R.; Alam, M. A. Screening-Limited Response of Nanobiosensors. *Nano Lett.* **2008,** *8*, 1281–1285.
20. Manz, A.; Graber, N.; Widmer, H. M. Miniaturized Total Chemical Analysis Systems: A Novel Concept for Chemical Sensing. *Sens. Actuators, B* **1990,** *1*, 244–248.
21. Petersen, K. E.; McMillan, W. A.; Kovacs, G. T. A.; Northrup, M. A. Toward Next Generation Clinical Diagnostic Instruments: Scaling and New Processing Paradigms. *Biomed. Microdev.* **1998,** *1*, 71–79.
22. Favier, F. E.; Walter, C.; Zach, M. P.; Benter, T.; Penner, R. M. Hydrogen Sensors and Switches from Electrodeposited Palladium Mesowire Arrays. *Science* **2001,** *293*, 2227–2231.
23. Penner, R. M. Mesoscopic Metal Particles and Wires by Electrodeposition. *J. Phys. Chem. B* **2006,** *106*, 3339–3353.
24. Steel, A. B.; Herne, T. M.; Tarlov, M. J. Electrochemical Quantitation of DNA Immobilized on Gold. *Anal. Chem.* **1998,** *70*, 4670–4677.
25. Hill, H. D.; Millstone, J. E.; Banholzer, M. J.; Mirkin, C. A. The Role Radius of Curvature Plays in Thiolated Oligonucleotide Loading on Gold Nanoparticles. *ACS Nano* **2009,** *3*, 418–424.
26. Bin, X.; Sargent, E. H.; Kelley, S. O. Nanostructuring of Sensors Determines the Efficiency of Biomolecular Capture. *Anal. Chem.* **2010,** *82*, 5928–5931.
27. Lapierre, M. A.; O'Keefe, M.; Taft, B. J.; Kelley, S. O. Electrocatalytic Detection of Pathogenic DNA Sequences and Antibiotic Resistance Markers. *Anal. Chem.* **2003,** *75*, 6327–6333.
28. Bernstein, J. A.; Khodursky, A. B.; Lin, P. H.; Lin-Chao, S.; Cohen, S. N. Global Analysis of mRNA Decay and Abundance in *Escherichia coli* at Single-Gene Resolution Using Two-Color Fluorescent DNA Microarrays. *Proc. Natl. Acad. Sci. U.S.A.* **2002,** *99*, 9697–9702.
29. Wang, H. Y.; Bhunia, A. K.; Lu, C. A Microfluidic Flow-Through Device for High Throughput Electrical Lysis of Bacterial Cells Based on Continuous DC Voltage. *Biosens. Bioelectron.* **2006,** *22*, 582–588.
30. Zhang, Y.; Pothukuchy, A.; Shin, W.; Kim, Y.; Heller, A. Detection of $\sim 10^3$ Copies of DNA by an Electrochemical Enzyme-Amplified Sandwich Assay with Ambient O_2 as the Substrate. *Anal. Chem.* **2004,** *76*, 4093–4097.
31. Vasilyeva, E.; Lam, B.; Fang, Z.; Minden, M. D.; Sargent, E.; Kelley, S. O. Direct Genetic Analysis of 10 Cancer Cells: Tuning Molecular Probe Design for Efficient mRNA Capture. *Angew. Chem., Int. Ed.*, in press, DOI: 10.1002/anie.201006793.